Tunable Resonator Implementation in Planar Groove Gap Waveguide Technology

Titus Oyedokun[1], Riana H. Geschke[1,2], Tinus Stander[3]

[1] Department of Electrical Engineering, University of Cape Town. South Africa.

[2] Fraunhofer Institute for High Frequency Physics and Radar Techniques FHR. Wachtberg, Germany.

[3] Carl and Emily Fuchs Institute for Microelectronics, Department of Electrical, Electronic and Computer Engineering, University of Pretoria. South Africa.

We present a tunable planar groove gap waveguide (PGGWG) resonant cavity at K_a*-band. The cavity demonstrates varactor loading and biasing without bridging wires or annular rings, as commonly is required in conventional substrate integrated waveguide (SIW) resonant cavities. A detailed co-simulation strategy is also presented, with indicative parametric tuning data. Measured results indicate a 4.48% continuous frequency tuning range of 32.52 to 33.98 GHz and a* Q_u *tuning range of 63 - 85, corresponding to DC bias voltages of 0 - 16V. Discrepancies between simulated and measured results are analysed, and traced to process variation in the multi-layer PCB stack, as well as unaccounted varactor parasitics and surface roughness.*

Keywords: Groove gap waveguide, planar waveguide, substrate integrated waveguide

Corresponding author: Titus Oyedokun;
email:oydtit001@myuct.ac.za

I. INTRODUCTION

There has been increased interest in frequency agile front-end components for mm-wave communication networks [1], as it provides the flexibility to select different frequency bands using the same infrastructure through post-fabrication tuning methods [1]. Substrate integrated waveguide (SIW) [2] frequency agile circuits have been demonstrated [3]-[5] but requires DC isolated planes for varactor biasing [6]. As a result, multiple etched annular rings [5] and bridging wires [3],[4] are required for biasing, with or without additional floating pads [5] that require connection through wire leads.

Planar groove gap waveguide (PGGWG) [7] features propagation characteristics similar to groove gap waveguide (GGWG [8]) in a planar PCB process similar to what is used for SIW. Unlike SIW, however, it provides the benefit of DC isolated conducting planes, which may be exploited for easy varactor biasing without the need for bridging wires as used in eg. [4]. It has also been shown that the resonant cavity Q-factor of PGGWG is comparable to SIW [7], but that PGGWG exhibits a slow-wave response compared to SIW, which aids in reducing the resonant cavity size [9]. This was previously demonstrated through broadband propagation studies of PGGWG [9] and fixed frequency resonators [7], but has yet to be explored in tuneable resonant cavities. The addition of varactor loading across the capacitive gap of the fixed frequency resonator in [7] would make the resonator tunable, but without the need for annular and bridging wires as is commonly required in varactor-loaded SIW tunable cavities.

This paper presents experimental results for a tunable K_a-band (commonly used for satellite communications and 5G base stations [10], radio astronomy [11] and cloud liquid water radiometry [12]) PGGWG resonant cavity exploiting the DC isolation advantage of the structure, using a simple varactor diode basing scheme previously analysed theoretically [13] [14]. We extend on the prior simulation study by presenting a detailed circuit-EM co-simulation model, providing measurement results, investigating discrepancies between simulated and measured results through detailed inspection of the multi-layer PCB stack-up (providing critical data for improved first-iteration modeling and prototyping accuracy for PGGWG development in future, which is not reported in [13],[14]) and systematically comparing the measured data to that of other approaches in the state-of-the-art literature.

II. TUNABLE PGGWG CAVITY GEMOMETRY

PGGWG is realised within parallel plate waveguide by using blind vias and catch pads to create an electromagnetic bandgap (EBG) medium on either side of a groove (Figure 1(a)) [7]. The groove allows for the propagation of TE_{10} mode similar to that in SIW. The EBG suppresses the parallel plate mode that would otherwise propagate along the sidewalls, similar to machined GGWG [15]. The advantage of biasing varactors using PGGWG is evident by the comparison in Figures 1(b) and 1(c). While a varactor-loaded combline cavity in PGGWG may be loaded using only conventional surface-mount components and etched DC traces, the loading of varactors in coaxial SIW cavities require a bridging wire and multiple annular rings. It is the bridging wires, in particular, that hamper mass production of the circuit, as it is a manufacturing step incompatible with automated pick-and-place PCB assembly. The disadvantage of PGGWG is that at least three copper routing layers are required, while SIW may be implemented on a single double-sided PCB. However, as multi-layer PCBs are commonly used for eg. SatCom applications [10], this is not necessarily a major drawback to the topology.

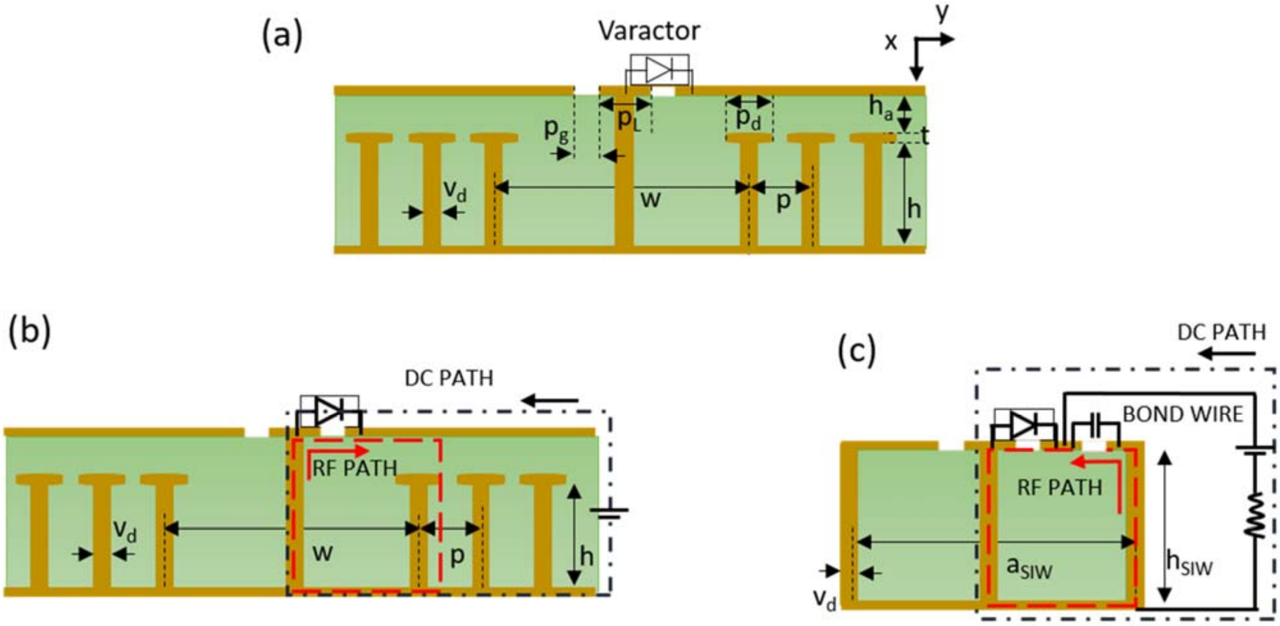

Figure 1. (a) Planar groove gap waveguide cavity cross-section. (b) RF and DC signal path in PGGWG rectangular resonant cavity. (c) RF and DC signal path in SIW resonant cavity [4].

The geometry of the rectangular tunable PGGWG cavity described here resembles a combline resonator topology, though the field pattern suggests a TE_{101} operating mode. The rectangular resonant cavity in Figure 2 uses 3 rows of EBG vias to form cavity sidewalls. This has been demonstrated to be sufficient to suppress parallel waves, ensuring that the field is confined within the groove [7]. The dimensions of the cavity are shown in Table 1. The non-PTFE, low-cost Mercurywave 9350 substrate with $\varepsilon_r = 3.5$ and loss tangent of 0.004 was used.

Table 1 Dimensions of the tunable PGGWG rectangular resonant cavity

Parameter	Value(mm)
w	5.48
h	0.508
h_a	0.168
v_d	0.3
p_d	0.7
p	0.95
p_L	0.75
p_g	0.15
t	0.017

The length of the cavity, L_g is chosen to ensure the fundamental TE_{101} mode resonates in the cavity while the coupling to the cavity, set by the iris width C_g, is chosen to minimize port loading effects, as is required by the three-point Q_0 extraction method [16]. The application of this technique requires light coupling (as seen in eg. Figure 5) and values of $S_{11} \approx 1$, leading to the approximation of $Q_0 \approx Q_e$ in extracting Q_0 from S-parameters. A through-hole plated via of diameter $v_d = 0.3$ mm is placed at the center of the cavity connecting the top isolated patch to the bottom conducting plane. The etched gap of width p_g ensures DC isolation despite the through-hole via in the middle of the cavity. The gap creates a capacitive loading between the centre post and the top metal layer of the PGGWG through the fringing fields across the gap. This can be observed in Figure 3 in the gap between the island patch and the top metal plate. As there is no experimentally defined definition of effective cavity width for PGGWG (as is available for SIW [18]), and since the analytically-defined coaxial resonant mode in [3] is not present here, the cavities are sized using full-wave parameter tuning.

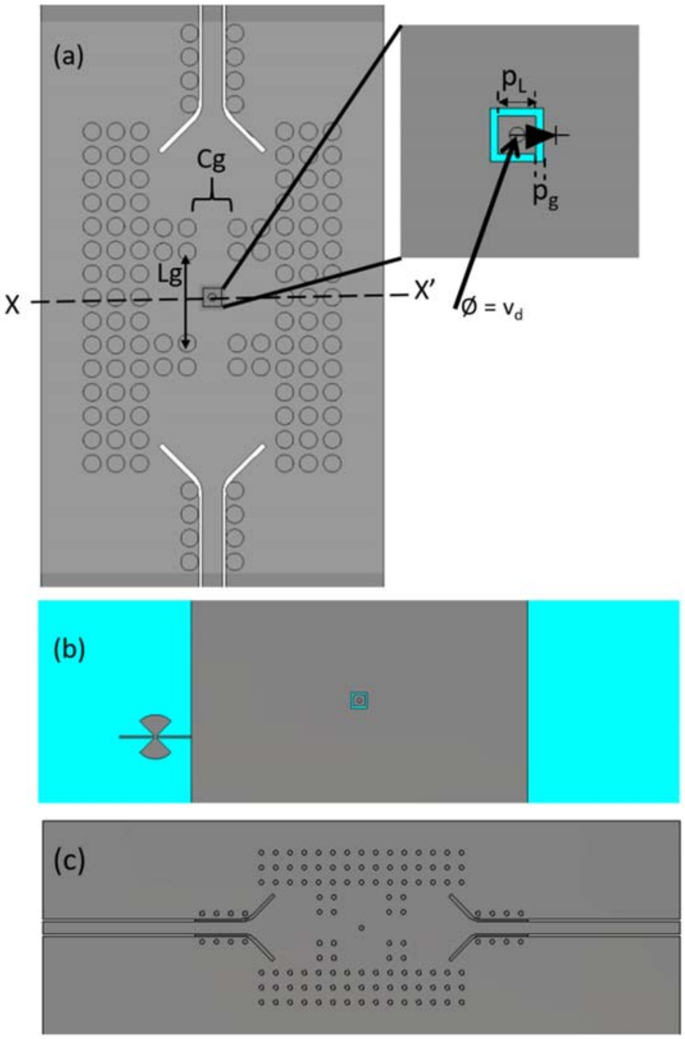

Figure 2. PGGWG rectangular resonant cavity structure. (a) Inside view of the cavity (b) Top view showing the center via and isolated metal patch and varactor diode attachment. (c) Bottom view.

Extensive parametric studies on the effects of p, h, v_d, and h_a variation on PGGWG have been presented previously [9,13]. The results of these parametric studies are applied here, to ensure that the band gap generated by the blind via rows (which effectively form the cavity sidewalls) covers the frequency range of the loaded TE_{101} resonant mode of the cavity, as determined by L_g (selected to be approximately $\lambda g/2$ at the required f_0, given the value of β reported in [9]) and w.

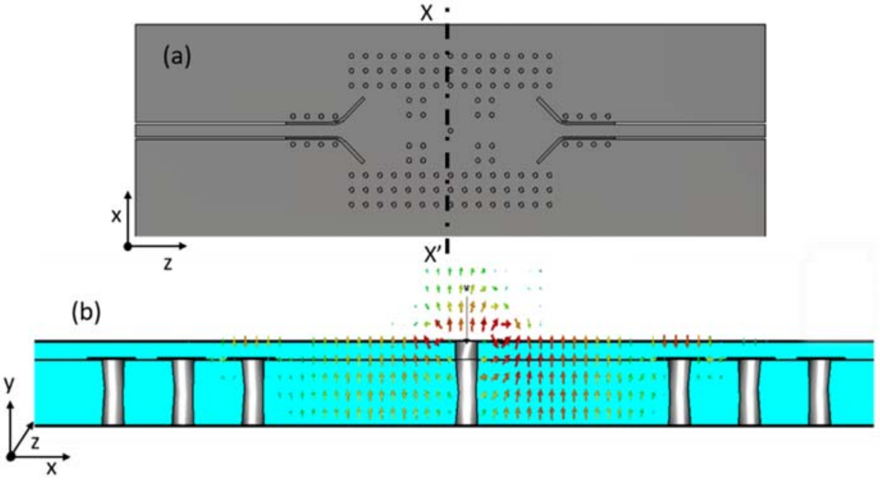

Figure 3 Electric field vector plot inside the cavity

A sequential multilayer printed circuit board build is applied in manufacturing the PGGWG. The EBG via holes are first drilled and plated on the substrate of height h, followed by through-hole plating and etching of the catch pads from the 17.5 µm copper cladding. The top substrate layer h_a is then added. The center via of the cavity is then drilled through the stack-up and through-hole plated, after which the floating pad is etched. As the center via is only drilled and plated after lamination, there is no risk for misalignment of separately drilled and plated vias (which may have been the case if the h and h_a substrates were drilled and plated separately prior to lamination). Consequently, there is no need for a catch-pad to provide for possible misalignment in the center via.

III. SIMULATION RESULTS

The loading capacitance C_g across the gap p_g of Figure 2 is controlled electrically by placing a varactor diode in reverse bias across the gap [13]. The varactor diode is biased by applying the DC voltage directly to the top conducting plane via a butterfly stub, which presents an RF open circuit at the point of contact with the top plate of the PGGWG cavity and an RF short circuit at the DC side of the stub.

An EM-circuit co-simulation is performed in CST Microwave Studio using the time domain solver as shown in Figure 4 A MACOM 46580 varactor diode is selected in this design example, with C_{jo} = 1.57pF. The parasitics of the varactor diode packaging, C_p and L_p are also included, as detailed in the manufacturer's datasheet.

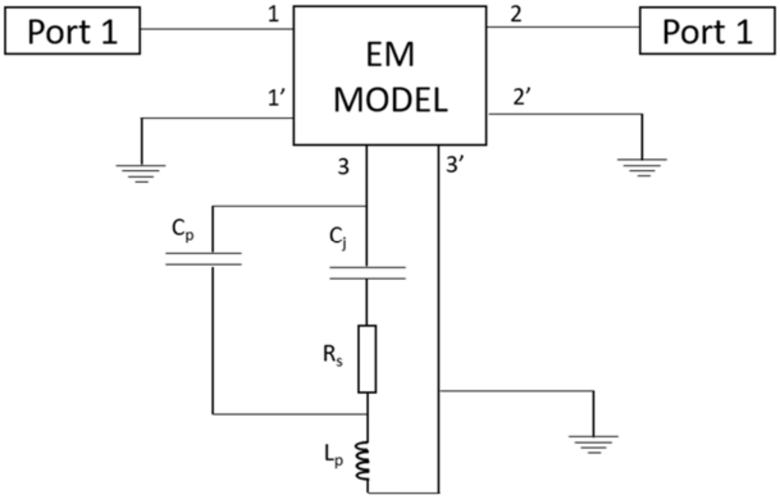

Figure 4. 3D EM-circuit co-simulation set-up showing the equivalent circuit model for MACOM 46461-276 varactor diode connected

Figure 5 shows the resulting S-parameters, which indicates a variation of f_0 from 31.63 to 32.71 GHz (3.36% tuning range) achieved by varying the junction capacitance from 0.15 pF to 0.45 pF. Neglecting surface roughness, the unloaded Q-factor varies over the tuning range from 143 to 160. In addition to the effect of parametric variations on h, v_d and p_d reported on previously [7]-[9] the parametric sweeps in Figures 6 and 7 indicates that the resonant frequency of the PGGWG cavity could be selected from a combination of parameters. In Figure 6 it can be observed that an increase in the width w (parameter indicated in Figure 1 decreases the resonant frequency of the cavity. Similarly, the changes in the cavity length L_g as shown in Figure 7 influences the resonant frequency of the cavity. The inverse relationship between f_0 and w, as well as L_g, support the view that the cavity exhibits a TE_{101}-type resonant mode, although the effective width a_{eff} is not well-defined as with SIW, which complicates an analytical calculation of f_0.

A variation in the square catch pad dimension, p_L is shown in Figure 7. A larger pad results in lower resonant frequency, due to an increased capacitive load to the PGGWG cavity. In comparison, variation in the via diameter, v_d, has a much smaller effect on resonant frequency, as shown in Figure 6

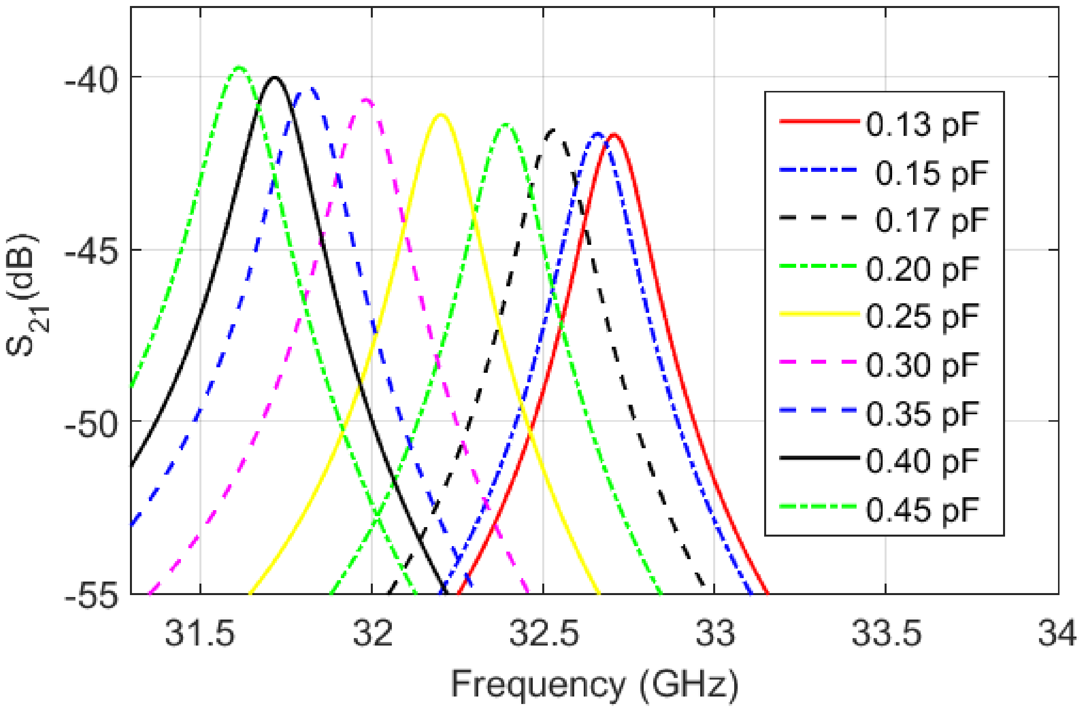

Figure 5 EM co-simulation result of S_{21} (dB) of the 2-port loaded rectangular PGGWG cavity.

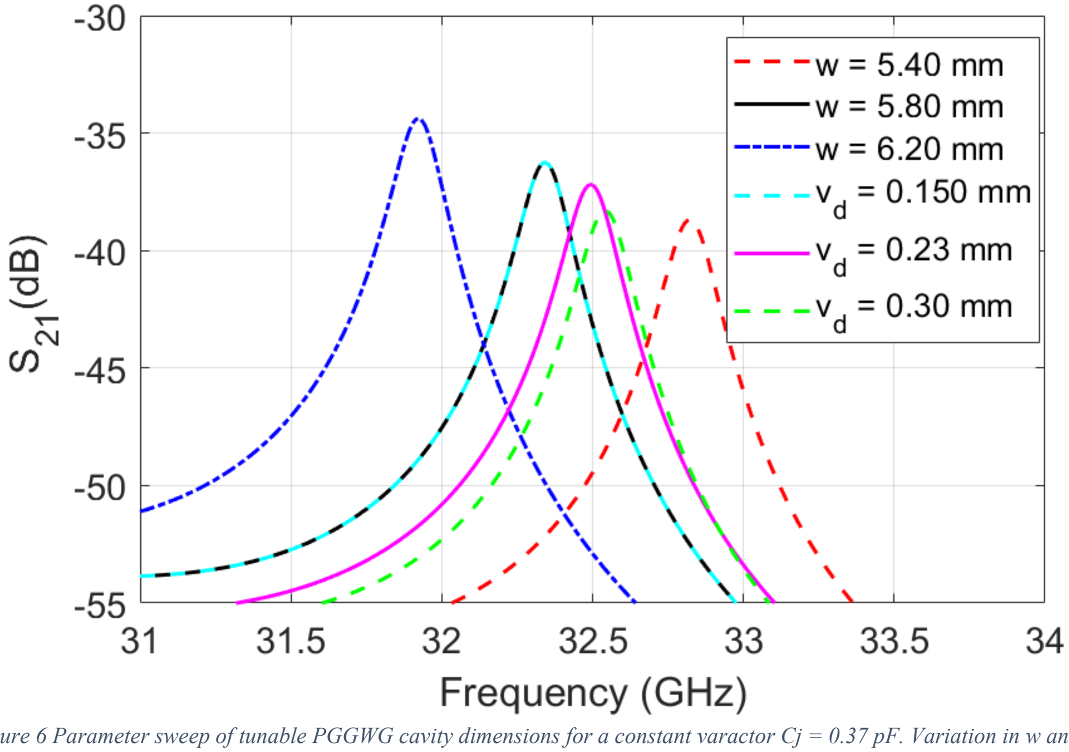

Figure 6 Parameter sweep of tunable PGGWG cavity dimensions for a constant varactor Cj = 0.37 pF. Variation in w and v_d shown.

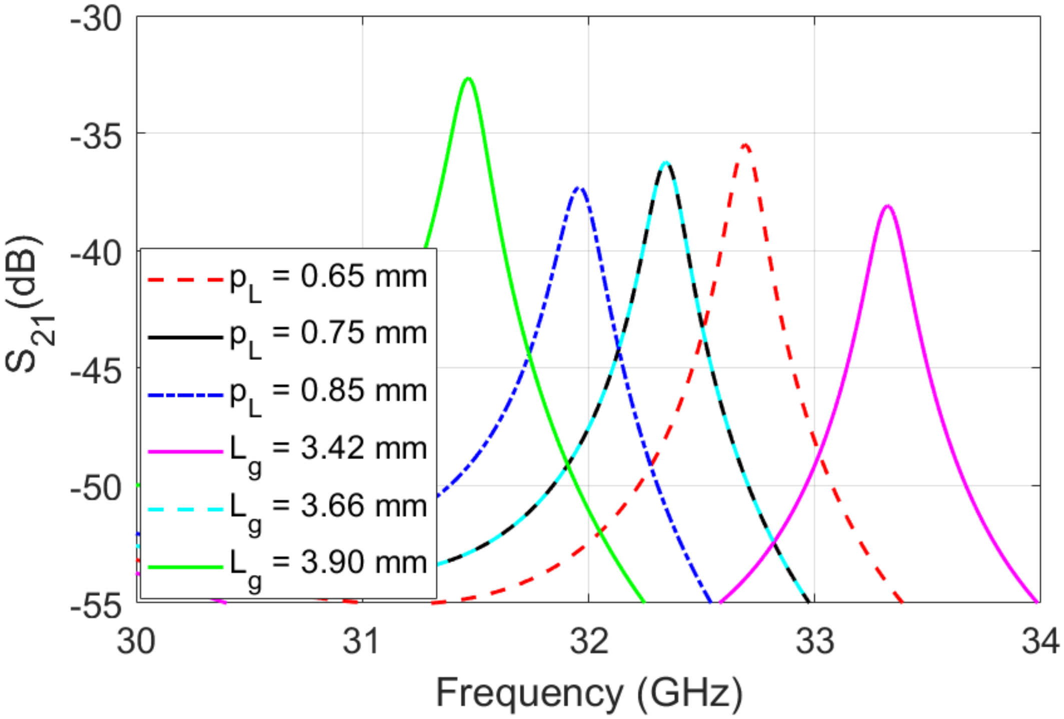

Figure 7 Parameter sweep of tunable PGGWG cavity dimensions for a constant varactor Cj = 0.37 pF. Variation of p_L and L_g.

IV. CONSTRUCTION AND MEASUREMENT RESULTS

Figure 8(a) and (b) shows the fabricated circuit (top and bottom view) with the varactor diode attached. Micrographs of sectioned views along the sidewall X_1-X_1' and along the center X-X' are shown in Figures 8(c) and 8(d), respectively.

The prototype is characterized on an Anritsu MS4647A VNA (Figure 9) The measured results in Figure 10 indicate a 4.48% continuous frequency tuning range from 32.52 to 33.98 GHz, corresponding to DC bias voltage range of 0 - 16V. The resonator Q_0 varies from 63 - 85 across the tuning range. Table 3 compares simulated and measured results.

After including 1.6µm RMS copper foil surface roughness [17] in the EM co-simulation of the tunable cavity, the discrepancy between simulated and measured Q-factors can be replicated, in simulation, by increasing R_S to 2.0 Ω (100% increase) resulting in an unloaded Q-factor of 76, or increasing tan δ to 0.01 (150% increase) with unloaded Q-factor of 87. These changes can be observed in Figures 11 and 12 The cause for the reduced Q-factor is, therefore, more likely to be underestimation of R_S in the circuit model than underestimation of tan δ.

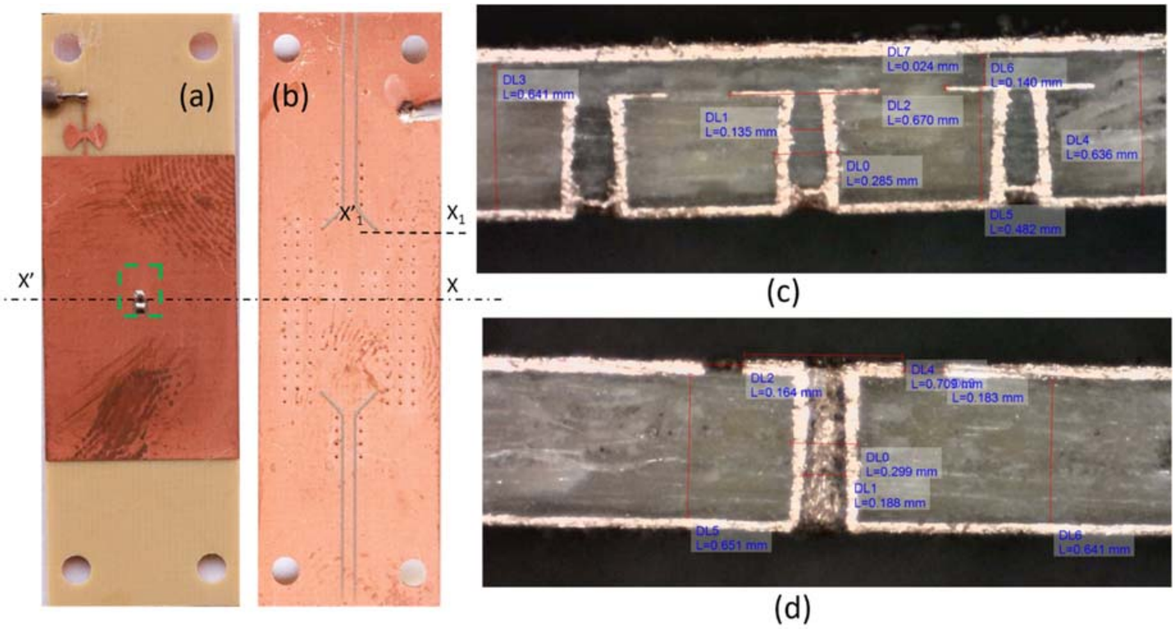

Figure 8 Photographs of the fabricated PGGWG tunable cavity circuit.(a) Top view with varactor diode attached. (b) Bottom view. (c) Micrographs showing the cross section X_1 –X'_1. (d) Micrographs showing the cross section X-X'. (e) Varactor diode attachment on the top plane. (f) DC bias line.

Table 2 A comparison between the dimensions of simulated and fabricated circuit

	Simulation (mm)	Fabricated (mm)	Error (µm)
h	0.508	0.482	26 µm (5.1%)
h_a	0.168	0.140	28 µm (16.6%)
p_d	0.7	0.670	30 µm (4.28%)
v_d	0.3	0.285	15 µm (5%)
p_L	0.75	0.709	41 µm (5.7%)
p_g	0.15	0.165	15 µm (10%)

The discrepancy between the simulated and manufactured geometries, as determined by micrograph, are shown in Table 2. This manufacturing errors can explain the shift in the resonant frequency of the circuit. A variation in the catch pad size p_d changes the resonance frequency of the cavity [9]. A decrease in the pad dimension increases the suppression band of the EBG, therefore increasing the resonant frequency of the cavity. Also, as observed in Table 3, the gap height h_a indicates a manufacturing error of 28 µm (16.6%). This changes the capacitance between the top conducting plane and the round catch pad, resulting in a shift of the suppression band of the PGGWG structure. Furthermore, the shift in frequency can also be attributed to an underestimation of the varactor parasitics in simulation. The 12 dB discrepancy between simulated and measured S_{21} maxima represents a variation of only 2.4% in transmission magnitude, and may safely be attributed to increased strength in coupling resulting from the reduced values of p_d and v_d. The three-point Q_0 characterization method [16] is not affected by this discrepancy, though this variation should be carefully considered in other applications where a specific Q_e is sought (eg. in filter or VCO circuits).

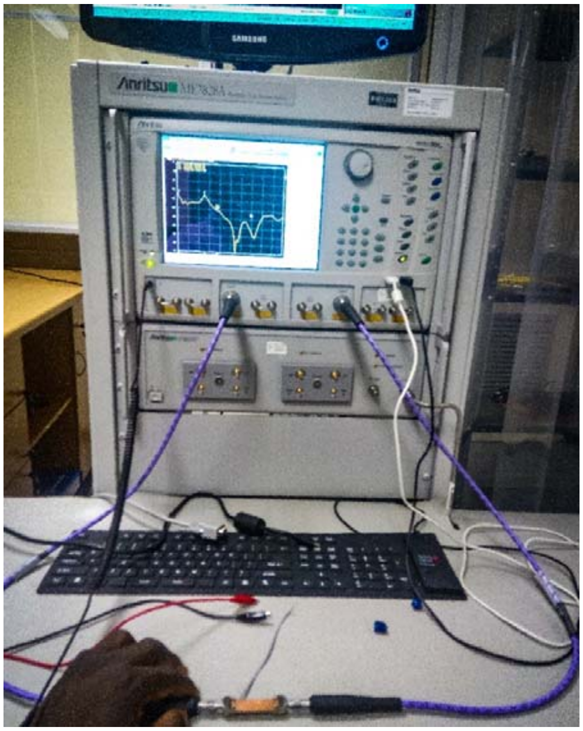

Figure 9 Photograph of the fabricated circuit attached to the Network Analyzer

Table 3 A comparison between simulated and measured results

	Simulation	Measurement
Frequency range (GHz)	31.61 - 32.53	32.52 - 33.98
Tuning range (%)	3.36	4.48
Q_u	143 - 160	463 - 85

Table 4 compares our work to the state-of-the-art in terms of achieved f_0, Q_0, tuning range, number of varactors used, and the necessity for bridging wires or multi-layer routing. S-parameters and external Q-factor Q_e are omitted from the comparison, as these are functions of resonator coupling (as determined by the synthesis of the application filter or VCO) and are not intrinsic performance metrics of the resonator itself [16]. From this table, it is evident that to enable varactor diode biasing, state-of-the-art schemes require multi-layer routing or bridging wires bridging wires or multi-layer routing, to which this work is an exception.

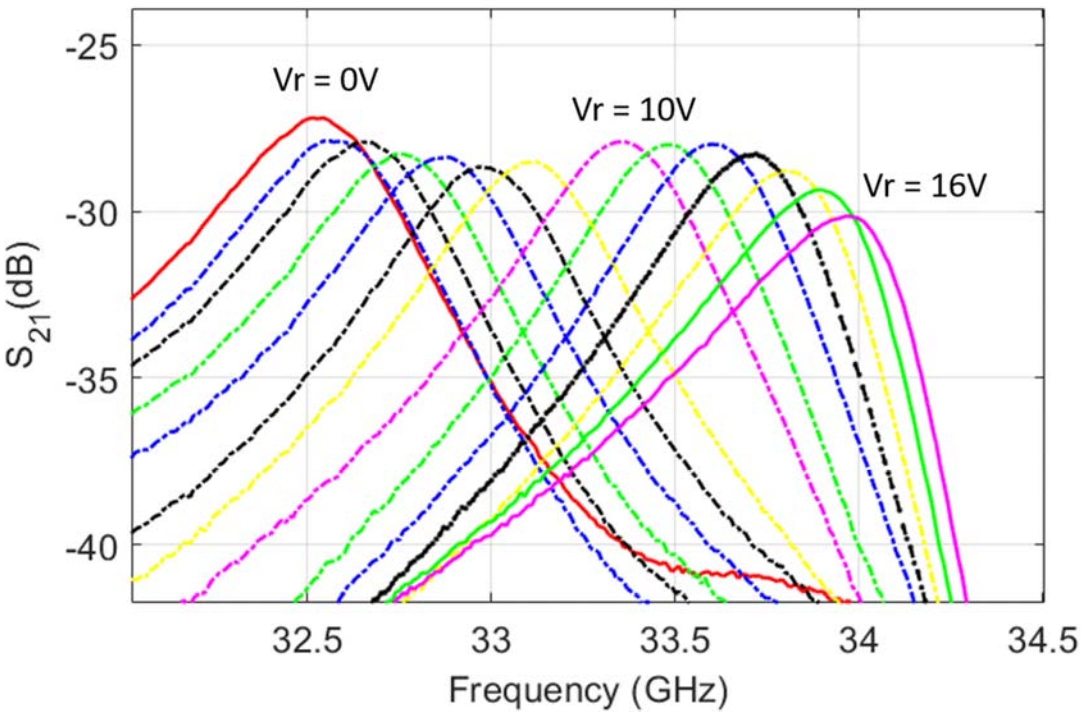

Figure 10 Measured S_{21}(dB) of the tunable PGGWG cavity

Table 4 Comparison of tunable resonant cavities

Ref	f_0 (GHz)	Q_0	Tuning range (%)	Number of varactors	DC routing
[19]	9.635	132-138	6.54	1	Bridging wires
[20]	13.03	N/A	1.23	1	Bridging wires
[4]	2.85	40-150	17.55	1	Bridging wires
[5]	0.82	90-214	73.17	20	Bridging lead resistors
[5]	2.22	35-100	55.86	1	Bridging lead resistors
[21]	2.1	280-296	28.57	1	Multi-layer routing
[22]	3.8/5.8	55	3.6	2	Bridging wires
[23]	11.6	286-299	4.3	1	Multi-layer routing
[24]	10	130-140	2.1	1	Bridging wires
This work	33.25	63-85	4.39	1	Uni-planar

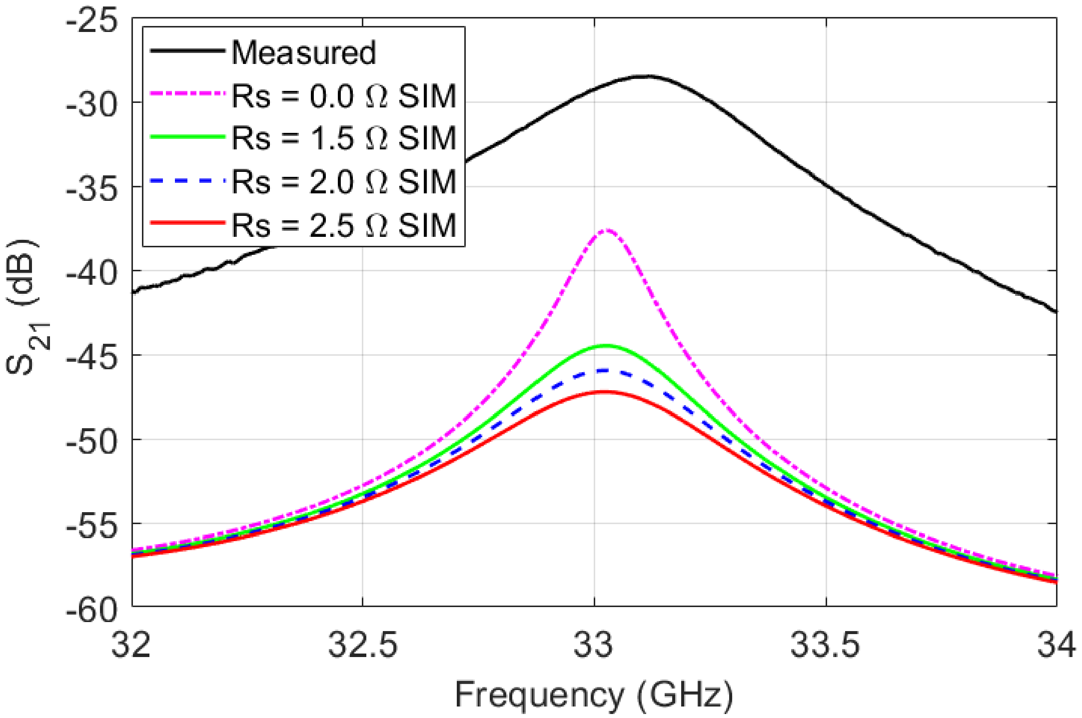

Figure 11 Comparison for Rs and tanδ with surface roughness 1.6$μm included in EM-co simulation of the tunable cavity. Rs is varied with C_{jo} = 0.37 pF, tanδ = 0.004

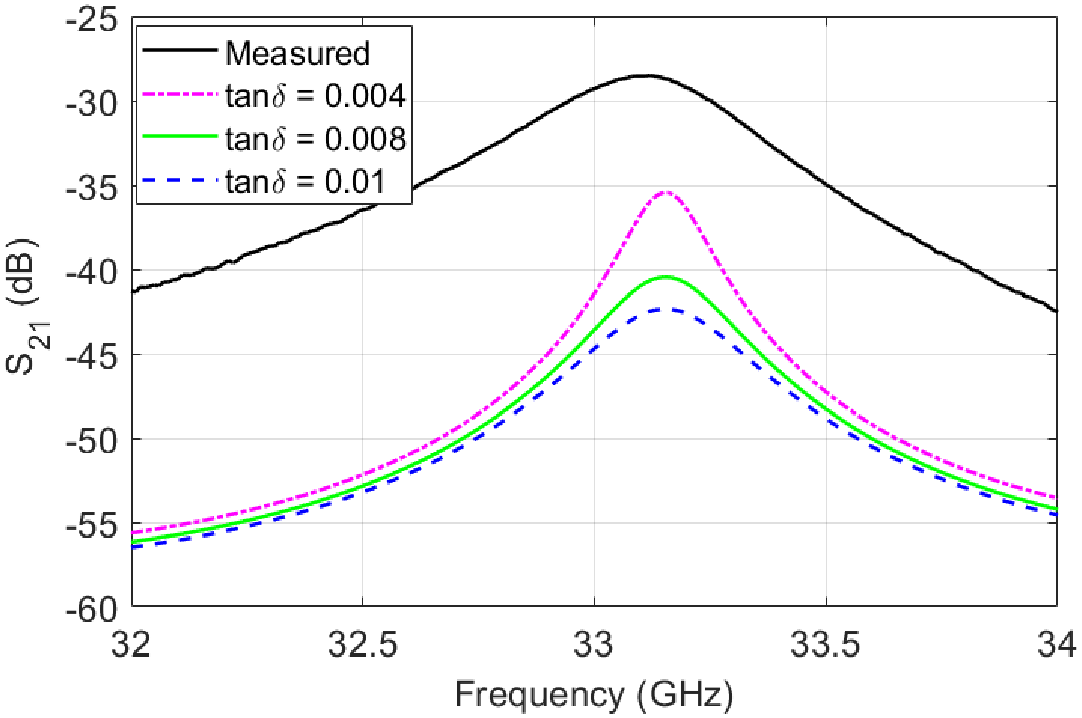

Figure 12 Comparison for Rs and tanδ with surface roughness 1.6μm included in EM-co simulation of the tunable cavity. tanδ is varied with Rs = 1.0Ω, C_{jo} = 0.37 pF.

V. CONCLUSION

Experimental validation of a tunable PGGWG resonant cavity is presented. This prototype demonstrates the benefit of PGGWG over SIW by exploiting the DC isolated conducting planes to bias a varactor diode, without annular rings or bridging wires to create a frequency agile combline resonator. Future work will extend this approach to other frequency agile applications, such as tuneable filters and voltage controlled oscillators (VCOs), establish analytical methods to synthesize the cavity, as well as experimental comparison with other planar guided media with similarly DC-isolated planes, eg. corrugated SIW [6].

ACKNOWLEDGEMENT

This work was supported in part by the National Research Foundation of South Africa (Scholarship 99870 and Grant number 88100).

REFERENCES

[1] Entesari K, A. P. Saghati, V. Sekar, and M. Armendariz, "Tunable SIW structures: Antennas, VCOs, and filters,"*IEEE Microwave Magazine*, 2015;16(1):34-54

[2] Bozzi M, A. Georgiadis and K. Wu, "Review of substrate-integrated waveguide circuits and antennas," *IET Microwaves,Antennas \& Propagation*, 2011;5(1)909-920.

[3] Sirci S, Martinez J, Taroncher M, Boria V. "Analog tuning of compact varactor-loaded combline filters in substrate integrated waveguide." *Proceeding of European Microwave Conference*, 2012;257-260

[4] Sirci S, Martinez JD, Taroncher M, Boria VE. "Varactor-loaded continuously tunable SIW resonator for reconfigurable filter design." *Proceeding of European Microwave Conference*, 2011; 436-439.

[5] Anand A, J. Small, D. Peroulis and X. Liu, "Theory and Design of Octave Tunable Filters With Lumped Tuning Elements" *IEEE Transactions on Microwave Theory and Techniques*, vol. 61, no. 12, pp. 4353-4364, Dec. 2013, doi: 10.1109/TMTT.2013.2287674

[6] Eccleston K.W, "Mode analysis of the corrugated substrate integrated waveguide," *IEEE Transactions on Microwave Theory and Techniques*, 2012; 60(1)3004-3012.

[7] Oyedokun T, Geschke R, Stander T. "Experimental characterisation of planar groove gap waveguide and cavity." *Proceeding of European Microwave Conference*, 2017;436-439. doi: 10.23919/EuMC.2017.8230883.

[8] Berenguer A, Fusco V, Zelenchuk D.E, Sánchez-Escuderos D, Baquero-Escudero M and Boria-Esbert V.E,"Propagation Characteristics of Groove Gap Waveguide Below and

Above Cutoff," *IEEE Transactions on Microwave Theory and Techniques*, vol. 64, no. 1, pp. 27-36, Jan. 2016, doi: 10.1109/TMTT.2015.2504501.

[9] Oyedokun, T, Geschke, RH, Stander, T. "Broadband mm-wave propagation characterization of planar groove gap waveguide." *Microw Opt Technol Lett*. 2020; 62: 1871– 1875. https://doi.org/10.1002/mop.32248

[10] Simon W. et al., "Highly Integrated Ka-Band Frontend Module for SATCOM and 5G," *IEEE Asia-Pacific Microwave Conference (APMC)*, Singapore, Singapore, 2019, pp. 441-443, doi: 10.1109/APMC46564.2019.9038880.

[11] Sitwala M,De Witt A, Van den Heever F, Malan S, Stander T, "Preliminary design of 18-45 GHz radio astronomy receiver," *Proc. SPIE 11453, Millimeter, Submillimeter, and Far-Infrared Detectors and Instrumentation for Astronomy X*, 1145348, December 2020; https://doi.org/10.1117/12.2562026

[12] Behrens M.T, Stander T, "Preliminary design of a dual 22/31 GHz single-chip water vapour radiometer," *Proc. SPIE 11445, Ground-based and Airborne Telescopes VIII*, 1144580, December 2020; https://doi.org/10.1117/12.2561999

[13] Oyedokun T, Geschke R and Stander T. "A Geometric study of tunable planar groove gap waveguide cavities." *IOP Conference Series: Materials Science and Engineering*, 2018; 321:012008.

[14] Oyedokun T, Geschke R and Stander T, "A tunable Ka-band planar groove gap waveguide resonant cavity," 2017 *IEEE Radio and Antenna Days of the Indian Ocean (RADIO*, Cape Town, 2017, pp. 1-2, doi: 10.23919/RADIO.2017.8242231.

[15] Rajo-Iglesias E, Kildal PS. "Groove gap waveguide: A rectangular waveguide between contactless metal plates enabled by parallel-plate cut-off." *Proceeding of European Conference on Antennas and Propagation*, 2010;1-4.

[16] Leong K and J. Mazierska, "Precise measurements of the Q factor of dielectric resonators in the transmission mode-accounting for noise, crosstalk, delay of uncalibrated lines, coupling loss, and coupling reactance," in *IEEE Transactions on Microwave Theory and Techniques*, vol. 50, no. 9, pp. 2115-2127, Sept. 2002, doi: 10.1109/TMTT.2002.802324.

[17] Liang T, Hall S, Heck H and Brist G, "A Practical Method for Modeling PCB Transmission Lines with Conductor Surface Roughness and Wideband Dielectric Properties," 2006 *IEEE MTT-S International Microwave Symposium Digest*, San Francisco, CA, 2006, pp. 1780-1783, doi: 10.1109/MWSYM.2006.249721.

[18] Caranicola R C, \& Fatima Salete. C ." 3.4/4.0 GHz Tunable Resonant Cavity in SIW Technology Using Metal Post and PIN Diode on a Low-Cost Biasing Network for 5G

Applications." *Journal of Microwaves, Optoelectronics and Electromagnetic Applications*, 19(1), 94-105. March 16, 2020.doi.org/10.1590/2179-10742020v19i11881

[19] He F, Wu K, Hong W, L. Han and Chen X, "A Low Phase-Noise VCO Using an Electronically Tunable Substrate Integrated Waveguide Resonator," *IEEE Transactions on Microwave Theory and Techniques*, vol. 58, no. 12, pp. 3452-3458, Dec. 2010, doi: 10.1109/TMTT.2010.2081550.

[20] He F, Chen X, Wu K and Hong W, "Electrically tunable substrate integrated waveguide reflective cavity resonator," *Asia Pacific Microwave Conference*, Singapore, 2009, pp. 119-122, doi: 10.1109/APMC.2009.5385418.

[21] Pourghorban A Saghati and K. Entesari, "A 1.7–2.2 GHz Compact Low Phase-Noise VCO Using a Widely-Tuned SIW Resonator," *IEEE Microwave and Wireless Components Letters*, vol. 24, no. 9, pp. 622-624, Sept. 2014, doi: 10.1109/LMWC.2014.2330502.

[22] Esmaeili M and Bornemann J, "Novel Tunable Bandstop Resonators in SIW Technology and Their Application to a Dual-Bandstop Filter with One Tunable Stopband," *IEEE Microwave and Wireless Components Letters*, vol. 27, no. 1, pp. 40-42, Jan. 2017, doi: 10.1109/LMWC.2016.2630007.

[23] Cariou M, Cadiou S, Potelon B, Quendo C, Ségalen R and Mahé F, "New tunable substrate integrated waveguide bandstop resonator," 2016 *IEEE MTT-S Latin America Microwave Conference (LAMC)*, Puerto Vallarta, 2016, pp. 1-3, doi: 10.1109/LAMC.2016.7851244.

[24] Chen Z, Hong W, Chen J and Zhou J, "Design of High-Q Tunable SIW Resonator and Its Application to Low Phase Noise VCO," *IEEE Microwave and Wireless Components Letters*, vol. 23, no. 1, pp. 43-45, Jan. 2013, doi: 10.1109/LMWC.2012.2234088.

Bibliographies

Titus Oyedokun. Titus Oyedokun received the B.Sc., M.Sc and Ph.D. in Electrical Engineering from the University of Cape Town, South Africa, in 2009, 2012 and 2019 respectively. In 2018, he joined Max Planck Institute for Radio Astronomy in Bonn Germany working as a research scientist on the development of cryogenic phased array feeds for radio telescope. His research focus is in planar waveguide technologies used in front-end radio receivers.

Riana H. Geschke. Riana Geschke's PhD research was on the topic of hybrid methods for computational electromagnetics. She was previously an Associate Professor at the University of Cape Town in South Africa, where her research activities were focused in the field of Applied Electromagnetics and Radio Astronomy systems. Since March 2019, she is a Research Scientist with the Fraunhofer Institute for High Frequency Physics and Radar Techniques (FHR) in Wachtberg, Germany.

Tinus Stander. Tinus Stander received the B.Eng. and Ph.D. degrees in electronic engineering from the University of Stellenbosch, Stellenbosch, South Africa, in 2005 and 2009, respectively. From 2010 to 2012, he served as an RF and Microwave Engineer at Denel Dynamics (a division of Denel SOC, Ltd.). He joined the Department of Electrical, Electronic,and Computer Engineering, Carl and Emily Fuchs Institute for Microelectronics, University of Pretoria, in 2013. He currently serves as a Principal Investigator in microwave and millimeter-wave microelectronics at the Institute, with personal research interest in the application of distributed passives on-chip and built-in self-testing. He is also registered as Professional Engineer with the Engineering Council of South Africa and serves as a Scientific Advisor with Multifractal Semiconductors (Pty) Ltd.